ELECTROLYTIC METHOD FOR OBTAINING POROUS CHITOSAN STRUCTURES WITH HYDROXYAPATITE

Michał Tylman*, Maria Mucha

Technical University of Lodz,
Faculty of Process and Environmental Engineering,
ul. Wolczanska 213, 90-924 Łódź, Poland
**e-mail: suppler1@o2.pl*

Abstract
The aim of this study was to develop a preparation method of porous chitosan structures, in the electrolysis of the chitosan solution in acetic acid. Chitosan in aqueous acetic acid is a polyelectrolyte. During the constant flow of electric current through this system, pure chitosan begins to accumulate on an anode, in the form of porous hydrogel layers. The addition of hydroxyapatite (HAp) to the electrolyte enhances the process and allows for obtaining spatially arranged complex structures of chitosan.

Key words: *electrolysis, electrolytic conductivity, chitosan, HAp.*

1. Introduction

Due to its biological properties, particularly the biocompatibility and bioactivity, chitosan has a great interest among researchers of biomedical fields. Studies on biopolymer systems based on chitosan in the form of a blend [1], scaffolds [2] or microspheres [3], are conducted in order to adapt them to the controlled release of drugs [4], implantation [5] or for dressings. Tissue engineering takes scaffolds, i.e. porous biodegradable polymer systems as a template for the regenerated tissue. The addition of various types of substances, including hydroxyapatite (HAp) [6], significantly increases the bioactive properties of the whole system, which can significantly shorten the time of bone tissue regeneration. Scaffolds for medical applications, depending on the desired porosity, are obtained by several processes, among which the most popular is the freeze evaporation of the solvent from the chitosan hydrogel or a chitosan acetate solution [7].

Systems thus obtained are characterized by the low mechanical strength, which precludes their direct use for example in bone implantation. In addition, chitosan acetate is soluble in water and without the pickling process in NaOH or crosslinking is rapidly degraded.

In the tissue environment, the problem of insufficient mechanical strength and structural changes of scaffold during pickling, causes the need to modify existing processes and to search for new ways to obtain scaffolds. In the literature there are few items concerning the process of electrolysis of a chitosan solution [8, 9]. In aqueous solution of acetic acid, chitosan is in the form of a polyelectrolyte. The flow of electric current through such a solution proceeds on the electrode with the separation of pure chitosan (water-insoluble). The addition of ions from the dissociation of HAp, significantly intensifies the process and allows for obtaining spatial structures, constituting the composite of chitosan-HAp. Such a system, after freeze-drying process can be used in bone tissue engineering, or in the technology of biosensors [10, 11].

2. Materials and methods

2.1. Materials

In the experiments chitosan (BioLog) of two degrees of deacetylation DD = 75% viscosity of 200 Pas and 85% and a viscosity of 120 Pas. Hydroxyapatite (HAp) $Ca_5(PO_4)_3OH$, for medical applications was produced by Sigma-Aldrich.

2.2 Methodology of the electrolysis

Electrolysis process was conducted in a glass vessel with a volume of 20 ml. Electrodes were made of stainless steel and their part immersed in an electrolyte was of dimensions 15 × 7 × 1 mm. The system was powered by a stabilized power supply for laboratory MNS – 300. The process was conducted at a constant voltage of 20 V, while the current depended on the instantaneous resistance of the electrolyte (in the process the resistance of the solution increased). ***Figure 1*** shows a diagram of electrolysis of chitosan in an acetic acid solution.

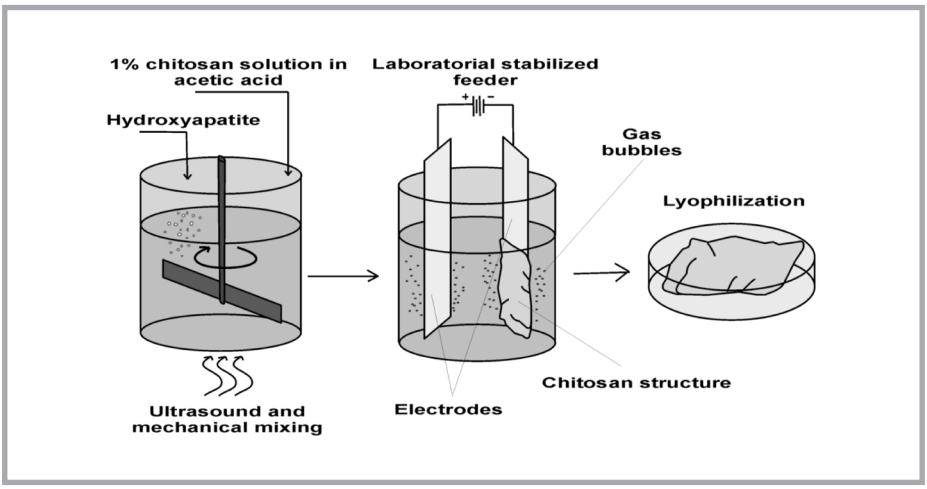

Figure 1. *Scheme of obtaining chitosan scaffolds in the process of electrolysis.*

To verify the effectiveness of the process depending on the composition of the electrolyte, the investigation was performed for 0.5 - 2% solutions of chitosan in 1% acetic acid The amount of hydroxyapatite added to the system (0 - 15%) changed as well.

2.3 Investigations of the conductivity of the solution

In the solution of a conductive electrolyte, electrical charge carriers are ions. The ability of an electrolyte to conduct electric current is determined by the conductivity of the electrolyte conductivity - χ.

$$\chi = 1/\omega = k/R_x \quad (1)$$

where:

χ - *electrical conductivity of the solution in S/m,*
ω - *resistivity of an electrolyte in* $\Omega \cdot m$,
R_x - *resistance of the solution,*
k - *constant of a conductometric vessel (k = L/S determined by a model solution, L – distance between the electrodes, S – area of an electrode).*

The measurement of electrical conductivity of the electrolyte in the experiment was performed using a laboratory conductometer DSP - 502, with a platinum electrode and a conductometric vessel. The conductivity measurement was made for the solutions of chitosan with different degrees of deacetylation, different concentration and the content of HAp.

2.4 Kinetics of electrolysis

Changes of current intensity were examined during the process. For measurement of the flowing current a laboratory ammeter, connected in parallel to the circumference of the electrode was applied. The scheme of the measurement system is shown in ***Figure 2***.

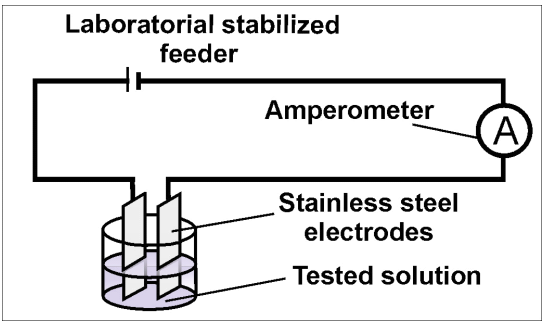

Figure 2. *The diagram of the system used to measure the current flowing through the electrolyte.*

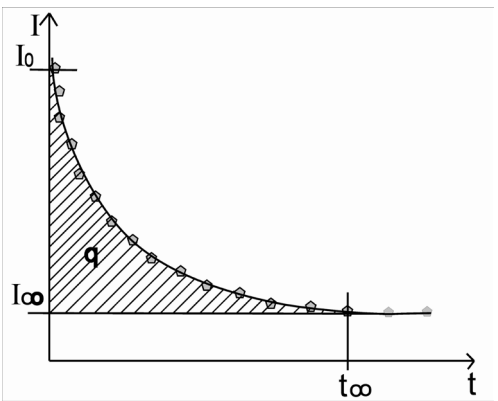

Figure 3. *Method of calculation of the charge flowing through the system up to the saturation time. Points – experimental, line – fitted curve by equation* $I = I_0 \cdot e^{-k}$*, symbols:* I_0 *– initial current,* I_∞ *- saturation current, q - electrical charge,* t_∞ *- saturation time.*

Masses of scaffolds removed from the electrode (after 5 minutes), were obtained in the process of electrolysis for the electrolyte with different contents of hydroxyapatite. The dry weight of scaffolds was also determined after drying to constant weight in a vacuum oven.

The electrical charge that flowed through the system until it reached saturation current (***Figure 3***) was determined, using ***Equation 2***. For the experimental points the exponential trend line was fitted. The area under the graph corresponds to the electrical charge, flowing through the system during the process.

The charge was calculated using Equation 2 as follows:

$$q = \int Idt = \int_{t=0}^{t=t_\infty} I_o e^{-kt}\,dt = \left[\frac{-I_o e^{-kt}}{k}\right]_{t=0}^{t=t_\infty} = \frac{-I_0}{k}\left[e^{-k\infty} - e^{-k\cdot 0}\right] = \frac{I_0}{k}\left[1 - e^{-k\infty}\right] = \frac{1}{k}\left(I_o - I_\infty\right) \quad (2)$$

where:

q –charge, I_0 – initial current, I_∞ - saturation current, k – constant, t – time.

2.5 Morphology of Samales

The structure of the scaffold obtained on the electrode was examined under an optical microscope of polarization-interference type for systems with different content of hydroxyapatite.

2.6 FTIR spectrum

The analysis of an infrared spectrum was performed for pure chitosan samples used in the experiment, and for the composite chitosan - HAp obtained in the process. The spectrum of pure hydroxyapatite in the KBr capsule was made as well. The study was performed using the Genesis II apparatus. The analysis of intermolecular interactions occurring in the analyzed composite was performed.

3. Results and disscusion

3.1 Electrical conductivity

There were carried out measurements of conductivity of solutions containing chitosan of different concentrations and two degrees of deacetylation, to examine their effects on the conductivity of the solution (***Figure 4.a***). Similarly, solutions with different HAp content were investigated (***Figure 4.b***). Figure 4 shows the dependence of the electrical conductivity on the solution concentration and the content of HAp.

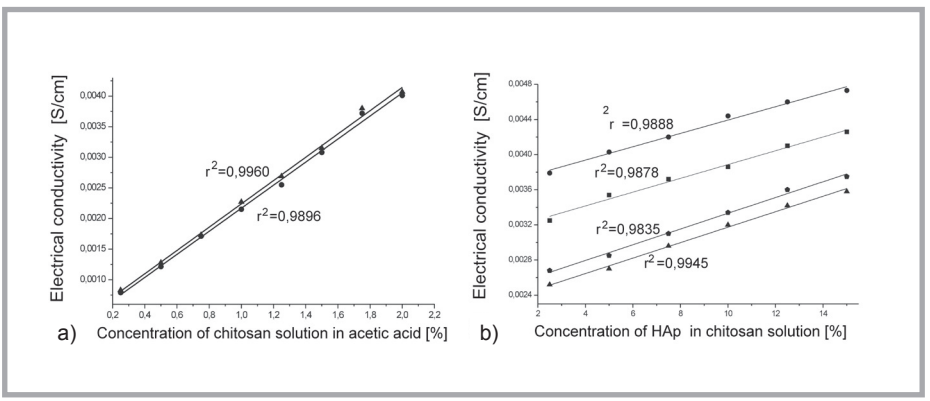

Figure 4. *Dependence of electrical conductivity on chitosan solution (a) hydroxyapatite solution (b); Symbols:* ***Figure a****: ▲- chitosan DD 85%,● – chitosan DD75%,* ***Figure b****: ● – 1.5% chitosan solution (DD 85%), ■ – 1.5% chitosan solution (DD 75%), ⬣ - 1% chitosan solution (DD 85%), ▲- 1% chitosan solution (DD 75%)*

The conductivity of the chitosan solution to a small extent depends on the degree of deacetylation. Increasing the concentration of the solution causes a linear increase in conductivity. The addition of hydroxyapatite, despite its low degree of dissociation, also increases the conductivity of the solution. It is related to the presence of additional Ca^{2+}, PO_4^{3-}, OH-, originating from the dissociation of hydroxyapatite.

3.2 Kinetics of the electrolysis

The current flowing through the system during the process was examined. The process of current flow can be divided into two periods. The first period comprises the rapid changes in intensity, occurring from the initial maximum current to the saturation current. During this period, changes occur exponentially and are associated with the intensive production of scaffold on the electrode. The resulting scaffold „clogs" the electrode, causing an increase in electrical resistance, and hence a sharp decrease in the intensity of the flowing current. ***Figure 5*** shows a diagram of the formation of chitosan scaffold on the cathode.

After this time, a second stage follows in which the current remains constant until the complete stop of the process associated with complete sealing of the electrode by the resulting scaffold. In the second stage, the active part of the electrode is connected with the pores of the scaffold.

The mass of the scaffolds obtained on the electrode depends on the duration of the process and the content of hydroxyapatite in the system. Hydroxyapatite significantly intensifies the process and allows for obtaining the spatially complex structures. ***Table 1*** summarized weights of scaffolds obtained on the electrode for 5 minutes of the process duration.

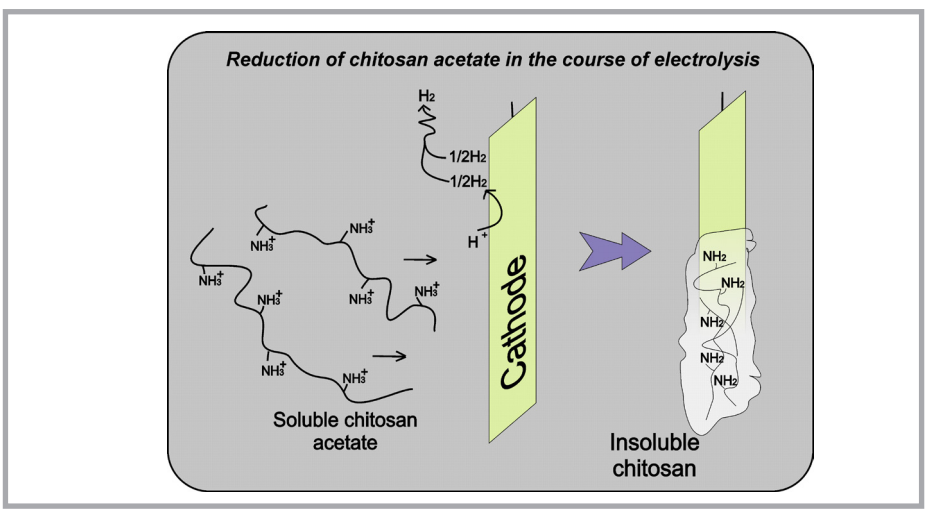

Figure 5. *The scheme of the process occurring on the cathode in the course of electrolysis.*

Table 1. *The dependence of scaffold weight obtained on the electrode on hydroxyapatite content in the electrolyte.*

Electrolyte	Weight of scaffold after 5 min. of the process, mg	Weight of dry scaffold, mg
Chitosan	10.3	8.5
Chitosan + 5% HAp	21.4	17.6
Chitosan + 10% HAp	67.3	52.6
Chitosan + 15% HAp	73.2	56.3

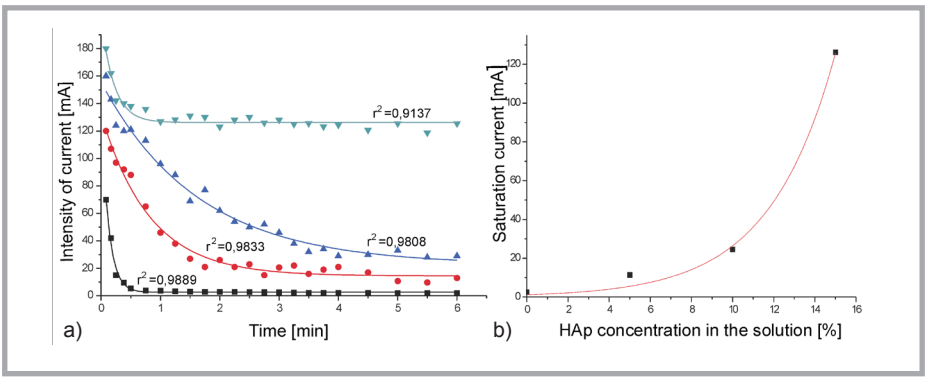

Figure 6. *Dependence of current on the duration time of the process (a), hydroxyapatite concentration in the solution (b); Symbols:▼ - 15% HAp in 1% chitosan solution in the acetic acid, ▲ - 10% HAp in 1% chitosan solution in the acetic acid, ● - 10% HAp in 1% chitosan solution in the acetic acid, ■ - 1% chitosan solution in the acetic acid.*

Figure 6 shows the dependence of current changes during the process (a) and the saturation current, depending on the amount of hydroxyapatite present in the system (b).

The charge of current flowing through the system, until achieving the saturation current. During the first period of current flow, until the saturation current, the largest mass of scaffold is set aside on the electrode. ***Table 2*** shows the dependence of the charge that flowed through the system (U = const = 20 V) in the first stage of the process, on the concentration of hydroxyapatite in the chitosan solution.

Table 2. *The electrical parameters of the system in dependence of HAp concentration in the electrolyte.*

Electrolyte	Maximum current I_0, mA	Saturation current I_∞, mA	Coefficient k, -	Charge q, C
Chitosan	71	4	7.35	0.017
Chitosan + 5% HAp	127	18	0.93	0.113
Chitosan + 10% HAp	160	38	0.47	0.270
Chitosan + 15% HAp	180	130	3.41	0.024

3.3 FTIR spectrophotometry

Figure 7 shows a spectrum for hydroxyapatite, chitosan and their composite with a marked displacement of the spectrum for the absorbance of NH group.

The analysis of the characteristic bands of chitosan spectrum, showed a band shift in the wavenumber 1560 [cm^{-1}], corresponding to the absorbance of the NH group. Band shift towards lower frequencies, shows some interactions between chitosan and hydroxyapatite, within that group. Changes are observed also in a broad band corresponding to OH oscillations. There are also changes in non-symmetric shape of this peak observed while passing towards lower frequencies, which indicates a change in the structure of hydroxyl bonds and participation of amino NH grups. The spectra should cover changes in the range of absorption band typical of phosphate ions PO_4 (about 550, 600 and 940 - 1320). It seems that changes in this range are significant but difficult to comment because of the interference of spectra. Like in the case of amino band, the range can be limited to local symmetry 1300 - 500 cm^{-1} corresponding to phosphate ions. More discussion on FTIR spectra results will be presented in a future.

3.4 Morphology of structures

Figure 8 shows a photograph of the swollen structure obtained on the electrode.

Scaffolds obtained on the electrode acquire the form of a porous hydrogel, the structure is compact and well hydrated (water content around 20%).

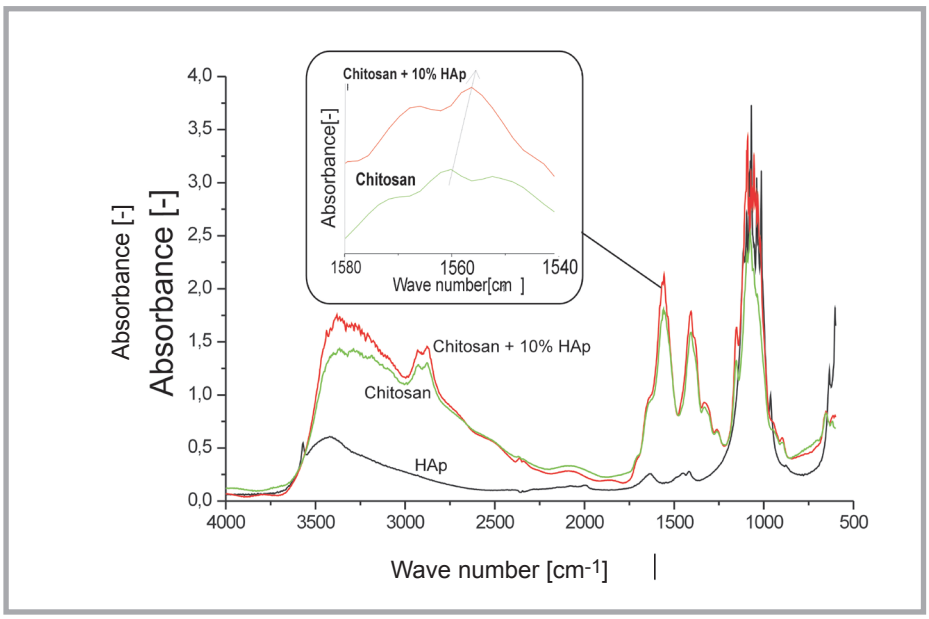

Figure 7. *FTIR spectrum: chitosan, hydroxyapatite and their composite.*

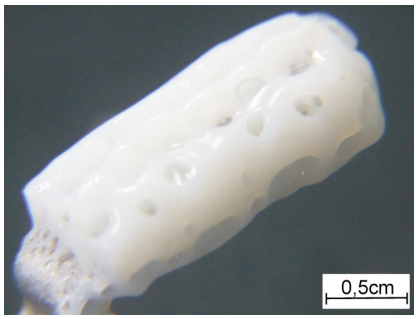

Figure 8. *The photograph of the structure obtained on the electrode in the course of electrolysis of a chitosan solution with 10% hydroxyapatite.*

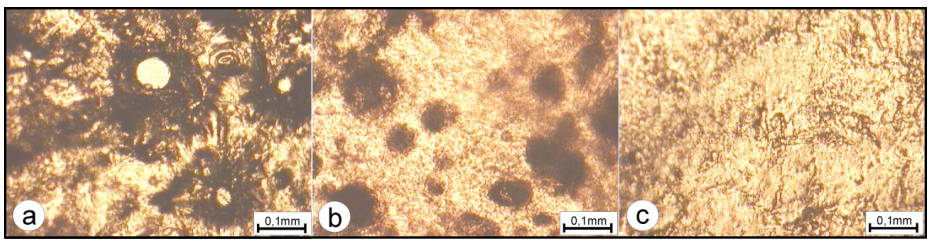

Figure 9. *The microphotograph showing swollen chitosan structures with a different HAp content: 5% (a), 10% (b), 15% (c).*

The pores in the system result from the release of gas (H_2) from the cathode in the electrolysis. After drying to constant weight in a vacuum oven, scaffold reduces its volume and becomes hard.

The analysis performed during the microscopic examination showed that the particles of hydroxyapatite are well disparged in the scaffold. This suggests that the resulting material can be a good medium for bone cell culture.

Figure 9 shows microphotographs of scaffolds, with different HAp content.

4. Conclusions

The composite of chitosan and hydroxyapatite was obtained in the electrolysis of solution of both compounds in acetic acid. The method of electrolysis, leading to a balanced combination of materials with properties such as chitosan (biocompatibility, bioactivity, and bacteria- and fungicidity) and hydroxyapatite (bioactivity in relation to bone cell - accelerating the process of osteogenesis), may be a good option for continually sought new biomedical materials, for implantation of bone. The research allowed to determine the best process conditions for the rapid manufacture of relatively large samples of the modified chitosan. Further research on this topic, will include understanding of the structure of the scaffold and its mechanical properties.

5. References

1. Scott P., Courtney H., Bumgardner J. D.; (2008) Chitosan Films: A Potential Local Drug Delivery System for Antibiotics. Clin Orthop. Relat. Res. Vol. 466, pp. 1377-1382.
2. Chen J., Nan K., Yin S.; (2010) Characterization and biocompatibility of nanohybrid scaffold prepared via in situ crystallization of hydroxyapatite in chitosan matrix. Colloids and Surfaces B: Biointerfaces, Vol. 81, pp. 640-647.
3. Chena X.-G., Liu Ch.-S., Liu C.-G.; (2006) Preparation and biocompatibility of chitosan microcarriers as biomaterial. Biochemical Engineering Journal, Vol. 27, pp. 269-274.
4. Sokker H. H., Ghaffar A. M., Gad Y. H., Aly A. S.; (2009) Synthesis and characterization of hydrogels based on grafted chitosan for the controlled drug release. Carbohydrate Polymers, Vol. 75, pp. 222-229.
5. Kong L., Gao Y., Lu G., Gong Y., Zhao N., Zhang X.; (2006) A study on the bioactivity of chitosan/nano-hydroxyapatite composite scaffolds for bone tissue engineering" European Polymer J, Vol. 42, pp. 3171-3179.
6. Sobczak A., Kowalski Z.; (2007) Materiały hydroksyapatytowe stosowane w implantologii. Czasopismo techniczne, Vol. 1, pp. 150-156.
7. Madihally V. S., Matthew H.; (1999) Porous chitosan scaffolds for tissue engineering. Biomaterials, Vol. 20, pp. 1133-1142.
8. Twu Y. K.,Chang I. T., Ping Ch.; (2005) Preparation of novel chitosan scaffolds by electrochemical process. Carbohydrate Polymers, Vol. 62, pp. 113-119.
9. LI Q., Song B., Yang Z., Fan H.; (2006) Electrolytic conductivity behaviors and solution conformations of chitosan in different acid solutions. Carbohydrate Polymers, Vol. 63, pp. 272-282.
10. Yi H., Wu L. Q., Bentley W. E., Ghodssi R., Rubloff G. W., Culver J. N., Payne G. E.; (2005) Biofabrication with Chitosan. Biomacromolecules, Vol. 6, pp. 2881-2891.
11. Qiu J. D., Xie H. Y., Liang R. P.; (2008) Preparation of porous chitosan/carbon nanotubes film modified electrode for biosensor application. Microchim Acta, Vol. 162, pp. 57-64.